Supporting Information

Exploring the robust engineered ω-transaminase for manufacturing biobased amines from biomass-derived aldehydes

Qi Li[a,b#], Junhua Di[a#], Zhengyu Tang[a#], Qing Li[b], Zhiyi Lu[a], Die Hu[a], Yu-Cai He[a,b*] and Cuiluan Ma[b]

[a] School of Pharmacy & School of Biological and Food Engineering, Changzhou University, Changzhou 213164, China

[b] State Key Laboratory of Biocatalysis and Enzyme Engineering, Hubei University, Wuhan 430062, China

* Correspondence: heyucai2001@163.com, yucaihe@cczu.edu.cn (Y.H.)

[#] They contributed equally to this work.

Supplementary Methods

S1. Construction of *E. coli At*TA and mutants

The gene encoding the ω-transaminase *At*TA from *Aspergillus terreus* was codon-optimized and synthesized. To construct the plasmid, primers pRSF-F and pRSF-R were used to linearize the pRSFDuet-1 backbone, while primers AT-F and AT-R amplified the *At*TA gene (Table S3, see SI). pRSFDuet-AT plasmid was obtained by homologous recombination of amplified *At*TA gene and linearized pRSFDuet-1 skeleton. The constructed plasmid (pRSFDuet-AT) was electroporated into competent *E. coli* BL21(DE3), generating a recombinant strain designated as *E. coli At*TA. To introduce site-directed mutations, a pair of short primers containing specific mutation sites (Table S4, see SI) were designed. The resulting mutants included: T130M, T130F, E133F, D134L, T130ME133F, T130MD134L, I77L, Q97E, H210N, N245D, G292D, H210NI77L, H210NQ97E, H210NN245D, H210NG292D, H210NI77LQ97E, H210NI77LG292D, H210NI77LQ97EN245D, and H210NI77LQ97EN245DG292D.

S2. Preparation of DES and synthesis of FAL and HMF

According to the predetermined molar ratio (Table S5, see SI), a precise amount of the hydrogen bond acceptor (HBA), such as betaine or choline chloride, and the hydrogen bond donor (HBD), including formic acid, lactic acid, urea, malic acid, malonic acid, glycerol, or ethylene glycol, was accurately weighed and added to a clean, dry 250 mL round-bottom flask. To initiate the synthesis, the flask was then placed on a magnetic stirrer with a heating function and maintained at a constant temperature of 80 °C while stirring at a speed of 260 rpm. Stirring continued until the solid components were completely dissolved, forming a homogeneous and transparent solution without any visible undissolved residues or precipitates, which indicated the successful formation of the deep eutectic solvent (DES). To ensure the stability of the system, the obtained DES solution was allowed to cool naturally to room temperature and subsequently transferred to a desiccator for further cooling, minimizing the influence of ambient humidity on its properties. Finally, the prepared DES was sealed and stored

in a dry, light-protected environment to prevent moisture absorption, oxidation, or degradation, thus ensuring its stability and suitability for subsequent experimental applications. FAL was synthesized by heating corncob (70 g/L) in a [ChCl][MA]-water mixture ([ChCl][MA] 30 vol%) at 160-180 °C for 10-30 minutes by autoclaving (400 rpm). Similarly, HMF was produced by heating bread crumbs (40 g/L) in the same [ChCl][MA]-water mixture under 170-190 °C for 15-90 minutes by autoclaving (400 rpm). Following the reactions, the mixtures were allowed to cool, then collected, diluted, and filtered prior to analysis by HPLC.

S3. Recycling and reuse of the DES system

The recyclability of [ChCl][MA] used in the HNILQEND-catalyzed reaction was evaluated through consecutive reuse experiments under the same conditions as the standard biocatalytic reactions. The initial reaction was performed in the [ChCl][MA]-containing aqueous system with whole-cell biocatalysts of *E. coli* HNILQEND, substrate, and amine donor at the optimized temperature and pH. After completion of each reaction cycle, the whole-cell biocatalyst was removed by centrifugation at 8000 rpm for 10 min. The supernatant was then subjected to liquid-liquid extraction using ethyl acetate to remove the reaction products. Following phase separation, the organic phase was discarded, and the remaining [ChCl][MA]-containing aqueous phase was collected. Fresh substrate, amine donor, and whole-cell catalyst were added to the recycled DES phase, and the reaction was conducted under identical conditions. This recycling procedure was repeated for multiple consecutive cycles. The catalytic performance of the recycled DES system was evaluated in each cycle by measuring product yield after a fixed reaction time. The performance in the first cycle was defined as the reference, and the relative catalytic activity in subsequent cycles was compared accordingly.

S4. Analytical method

An LC-2030C (3D) HPLC system (SHIMADZU Co., Japan) equipped with a Discovery C18 column (25 cm × 0.46 cm, 5 μm) was used for analysis. The mobile phase consisted of 20 vol % CH_3OH, 80 vol % H_2O containing 0.1 wt% TFA, delivered at a flow rate of 0.8 mL/min and maintained at 35 °C. FAL and HMF were monitored

at a detection wavelength of 254 nm, while FLA and HMFA were detected at 210 nm.

Supplementary Tables

Table S1. Half-life and kinetic parameters of the ω-transaminase *At*TA and HNILQEND.

ω-Transaminase	$t_{1/2}^{50°C}$, h	$t_{1/2}^{35°C}$, h	K_m, mM	V_{max}, mM/min	K_{cat}, s^{-1}
*At*TA	0.41	10.03	95.01	0.62	1.56
HNILQEND	2.38	125.02	50.37	0.72	1.80

Table S2. Data collection and refinement statistics for the crystal structure of HNILQEND.

Parameters	HNILQEND
PDB ID	8XIY
Data collection	
SSRF beamline	BL19U1
Wavelength (Å)	0.9786
Space group	*C 2 2 21*
Resolution (Å)	2.09 (41.88-2.09)
a, *b*, *c* (Å)	106.42, 135.79, 116.93
α, *β*, *γ* (degrees)	90.00, 90.00, 90.00
Subunits in asymmetric unit	2
No. of unique reflections	49080
Data completeness %	97.4 (48.11-2.09)
R_{merge}	0.104
$R_{p.i.m.}$	0.034
Anisotropy	0.083
Average $I/\sigma(I)$	2.37 (at 2.08 Å)
Refinement	
R_{work}/R_{free} (%)	17.1/21.6
B from Wilson plot (Å^2)	28.4
R_{free} test set	2416 reflections (4.93%)
No. of protein atoms	5530
No. of water atoms	497
No. of ligand atoms	47
Average *B* value, all atoms (Å^2)	29.0
RMSD bond lengths (Å)	0.42
RMSD bond angles (degrees)	0.56
Ramachandran plot favored (%)	98%
Ramachandran plot allowed (%)	2%
Ramachandran plot outlier (%)	0%

Table S3. Strain, plasmids, and primer used in this study.

Strain, plasmid or primer	Description or sequence (5'-3')	Source
Strain		
Escherichia coli DH5α	gene cloning strain	Novagen (Shanghai, China)
Escherichia coli BL21 (DE3)	protein expression strain	Novagen (Shanghai, China)
Plasmid		
pRSFDuet-1	Kan^+	Novagen (Germany)
Primer		
AT-F	GCCATCACCATCATCACCACATGGCCA GCATGGATAAAGTTTTTG	Sangon (Shanghai, China)
AT-R	GCTCGAATTCGGATCCTGGCTTAATTG CGTTCGTTATAATCGATCTCAAAGC	
pRSF-F	AGCCAGGATCCGAATTCGAGC	Sangon (Shanghai, China)
pRSF-R	GTGGTGATGATGGTGATGGCTGC	

Table S4. Primers containing mutation sites used in this study.

Mutation	Template	Primers (5'-3')
T130M	pRSFDuet-AT	Forward: GTCTGAAAGGTGTTCGTGGCATGCGTCCGGAAGAT ATTGTTAA Reverse: CCGGTGTATACAGAACGCCATCTTTAACCAGAACA ATGTTAAAACCGC
T130F	pRSFDuet-AT	Forward: GTCTGAAAGGTGTTCGTGGCTTCCGTCCGGAAGAT ATTGTTAA Reverse: CCGGTGTATACAGAACGCCATCTTTAACCAGAACA ATGTTAAAACCGC
E133F	pRSFDuet-AT	Forward: CGTGGCACCGTCCGTTCGATATTGTTAATAATC Reverse: CCGGTGTATACAGAACGCCATCTTTAACCAGAACA ATGTTAAAACCGC
D134L	pRSFDuet-AT	Forward: CGTGGCACCCGTCCGGAATTAATTGTTAATAATCT GTAT Reverse: CCGGTGTATACAGAACGCCATCTTTAACCAGAACA ATGTTAAAACCGC
T130M/E133F	pRSFDuet-T130M	Forward: CGTGGCATGCGTCCGTTCGATATTGTTAATAATC Reverse: CCGGTGTATACAGAACGCCATCTTTAACCAGAACA ATGTTAAAACCGC
T130M/D134L	pRSFDuet-T130M	Forward: CGTGGCATGCGTCCGGAATTAATTGTTAATAATCT GTAT Reverse: CCGGTGTATACAGAACGCCATCTTTAACCAGAACA ATGTTAAAACCGC
I77L	pRSFDuet-AT	Forward:

		CTGGATGATCATTTAACCCGTCTGGAAGCAAGCTG TACCAAACTGC Reverse: GTACGTGCAACAACTGCGCTACCACCAACACGCT G
Q97E	pRSFDuet-AT	Forward: GCCGCTGCCTCGTGATGAGGTTAAACAAATTCTGG TTGAAATGG Reverse: CAGATCACCCCACTGCAGATTTTTAACGGTCGGAT CAATTGCACC
H210N	pRSFDuet-AT	Forward: CTGACCGATGGTGATGCAAATCTGACCGAAGGTA GCGG Reverse: CCAATCTGACCACCATTAACCGGCATACCATCCAG TGTGG
N245D	pRSFDuet-AT	Forward: CCCGTAAAAGCGTTATTGATGCAGCAGAAGCCTTT GGTATTGAAGTG Reverse: CCGAGCTCGAATTCGGATCCTGGCTTAATTGCGTT CG
G292D	pRSFDuet-AT	Forward: GGATGGTATGCCGGTTAATGATGGTCAGATTGGTC CGATCACC Reverse: CTAAGATGGGGAATTGTTATCCGCTCACAATTCCC CTATAGTGAGTCG
H210N/I77 L	pRSFDuet-H210N	Forward: CTGGATGATCATTTAACCCGTCTGGAAGCAAGCTG TACCAAACTGC Reverse: GTACGTGCAACAACTGCGCTACCACCAACACGCT G
H210N/Q97 E	pRSFDuet-H210N	Forward: GCCGCTGCCTCGTGATGAGGTTAAACAAATTCTGG TTGAAATGG Reverse: CAGATCACCCCACTGCAGATTTTTAACGGTCGGAT CAATTGCACC
H210N/N24 5D	pRSFDuet-H210N	Forward: CCCGTAAAAGCGTTATTGATGCAGCAGAAGCCTTT GGTATTGAAGTG

		Reverse: CCGAGCTCGAATTCGGATCCTGGCTTAATTGCGTTCG
H210N/G292D	pRSFDuet-H210N	Forward: GGATGGTATGCCGGTTAATGATGGTCAGATTGGTCCGATCACC Reverse: CTAAGATGGGGAATTGTTATCCGCTCAC
H210N/I77L/Q97E	pRSFDuet-H210N/I77L	Forward: GCCGCTGCCTCGTGATGAGGTTAAACAAATTCTGGTTGAAATGG Reverse: CAGATCACCCCACTGCAGATTTTTAACGGTCGGATCAATTGCACC
H210N/I77L/G292D	pRSFDuet-H210N/I77L	Forward: GGATGGTATGCCGGTTAATGATGGTCAGATTGGTCCGATCACC Reverse: CTAAGATGGGGAATTGTTATCCGCTCACAATTCCCCTATAGTGAGTCG
H210N/I77L/Q97E/N245D	pRSFDuet-H210N/I77L/Q97E	Forward: CCCGTAAAAGCGTTATTGATGCAGCAGAAGCCTTTGGTATTGAAGTG Reverse: CCGAGCTCGAATTCGGATCCTGGCTTAATTGCGTTCG
H210N/I77L/Q97E/N245D/G292D	pRSFDuet-H210N/I77L/Q97E/N245D	Forward: GGATGGTATGCCGGTTAATGATGGTCAGATTGGTCCGATCACC Reverse: CTAAGATGGGGAATTGTTATCCGCTCACAATTCCCCTATAGTGAGTCG

Table S5. Synthesis of the deep eutectic solvents.

DES	HBA	HBD	Molar ratio
[ChCl][FA]	choline chloride	formic acid	1:1
[ChCl][LA]	choline chloride	lactic acid	1:1
[ChCl][MAC]	choline chloride	malic acid	1:1
[ChCl][MA]	choline chloride	malonic acid	1:1
[ChCl][Urea]	choline chloride	urea	1:2
[ChCl][Gly]	choline chloride	glycerol	1:2
[ChCl][EG]	choline chloride	ethylene glycol	1:2
[BA][LA]	betaine	lactic acid	1:2
[BA][MA]	betaine	malonic acid	1:2

Supplementary Figures

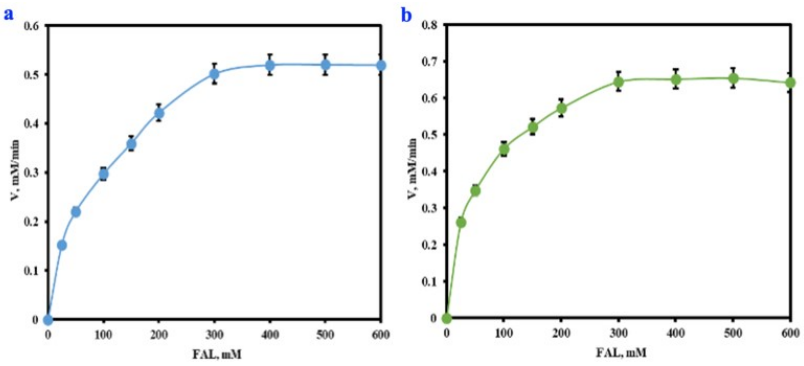

Fig. S1 Michaelis-Menten fitting curves of the wild-type (a) and HNILQEND (b).

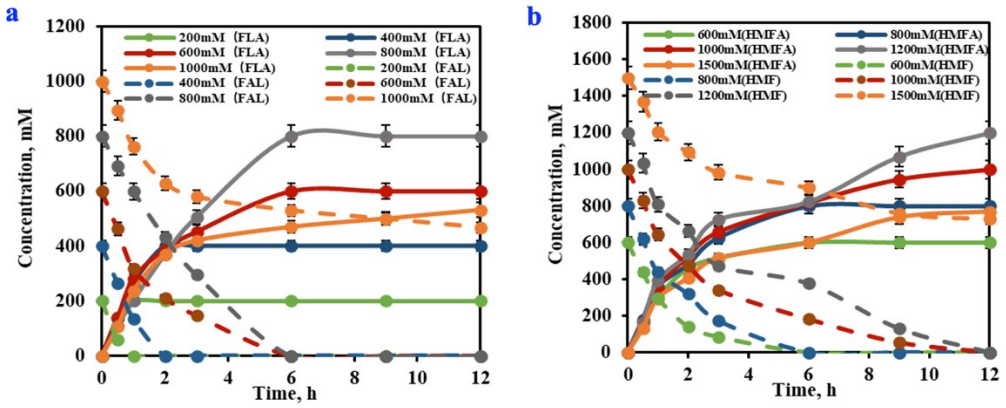

Fig. S2 The substrate tolerance of HNILQEND towards varying concentrations of FAL (a) and HMF (b).

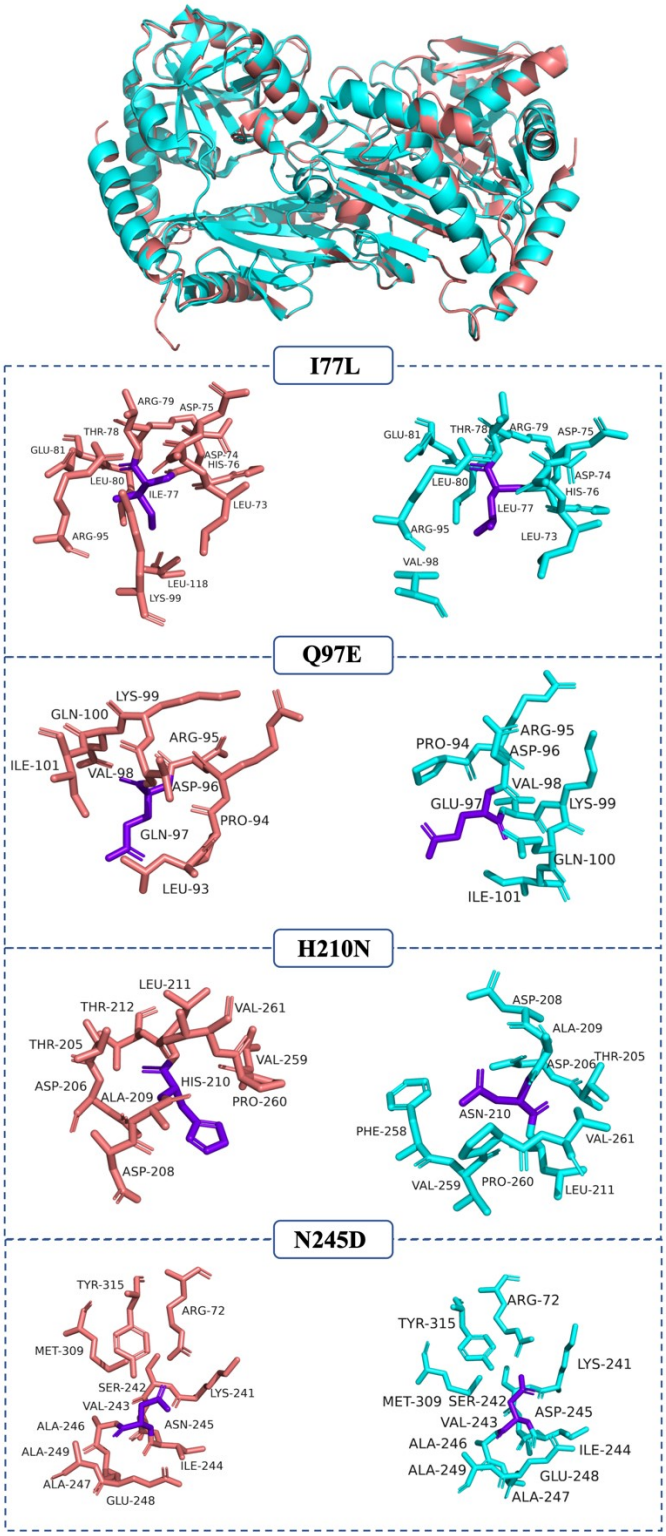

Fig. S3 Structural comparison of local environments around the mutation sites within a 4 Å radius in the wild-type and HNILQEND [The wild-type enzyme is shown in red, whereas the HNILQEND mutant is shown in blue].

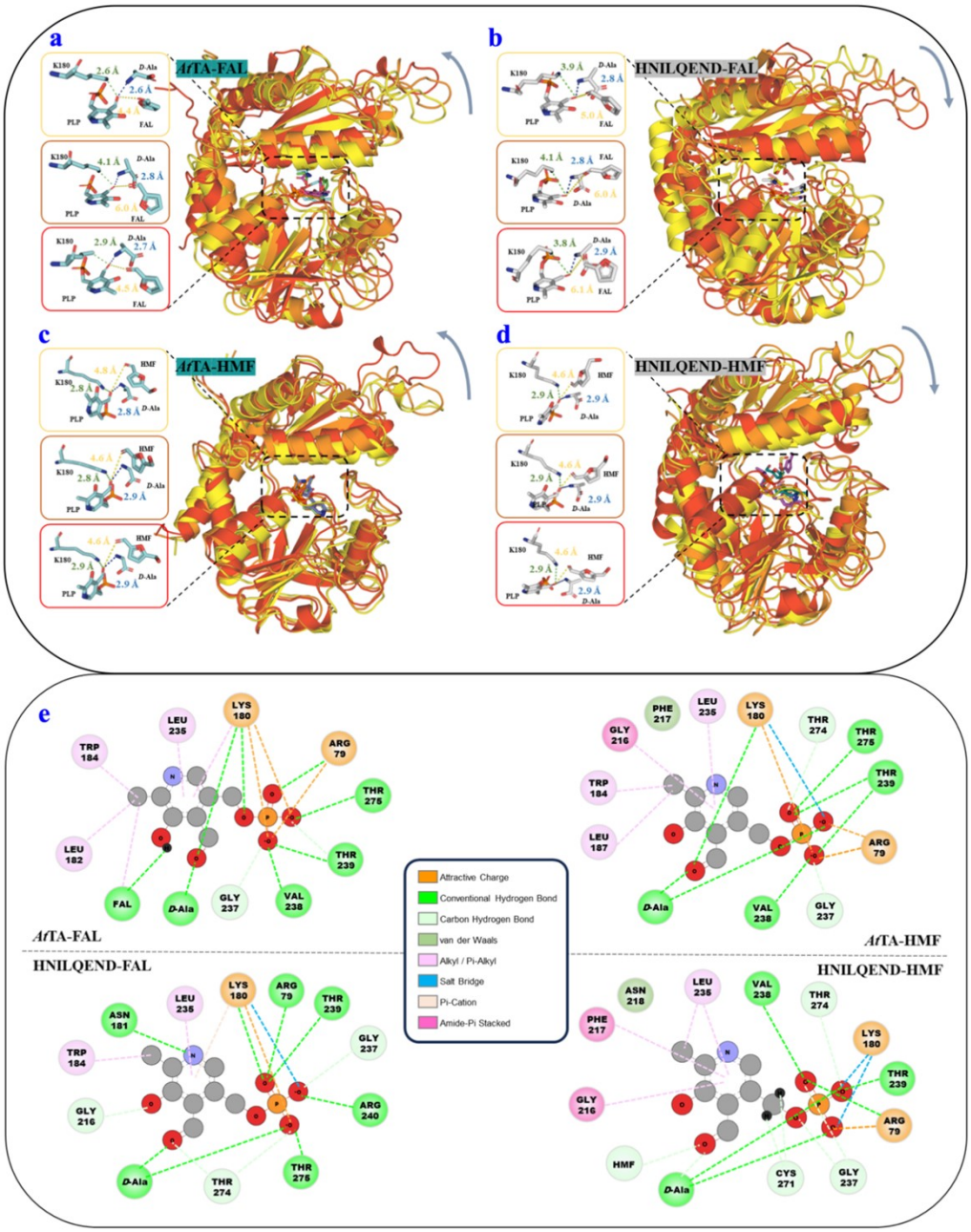

Fig. S4 Conformational dynamics of substrate-gating loops and substrate-cofactor geometry: *At*TA -FAL representative conformers with upward displacement of the substrate-gating loop (a), HNILQEND-FAL conformers showing downward displacement of the substrate-gating loop (b), *At*TA-HMF conformers with retracted loop motion (c), HNILQEND-HMF conformers exhibiting repositioned loop orientation (d) [Insets: Catalytic pocket distances labeled for K180-PLP, *D*-Ala-PLP, and substrate-PLP in each cluster]; Non-bonded interaction networks in catalytic pockets (e).

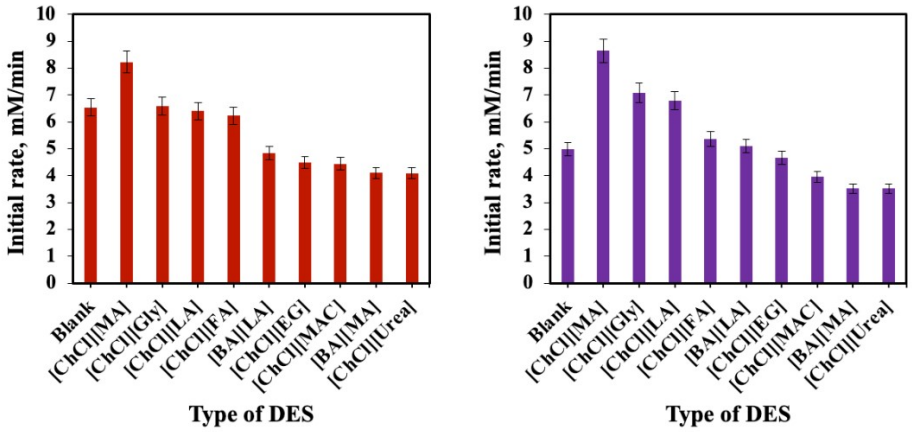

Fig. S5 Effect of DES type on HNILQEND catalysis of FAL (a) and HMF (b).

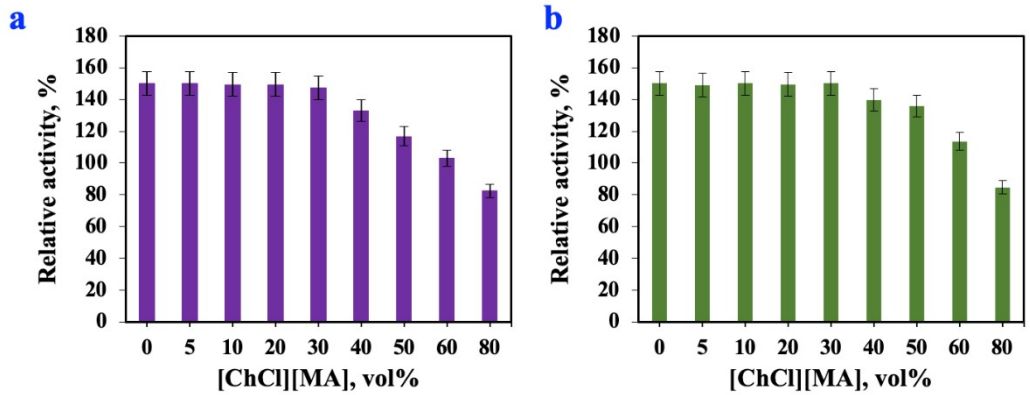

Fig. S6 The effect of varying [ChCl][MA] content in the reaction solvent system on HNILQEND catalysis of FAL (a) and HMF (b).

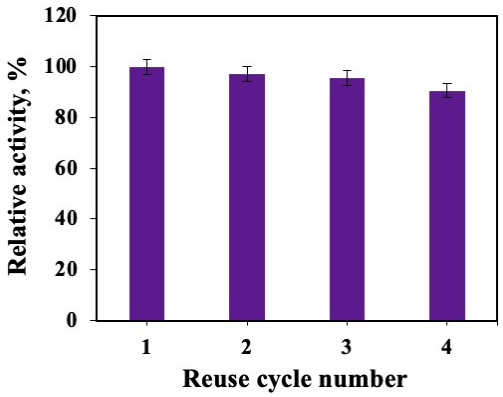

Fig. S7 Reusability of [ChCl][MA] in the HNILQEND-catalyzed reaction.

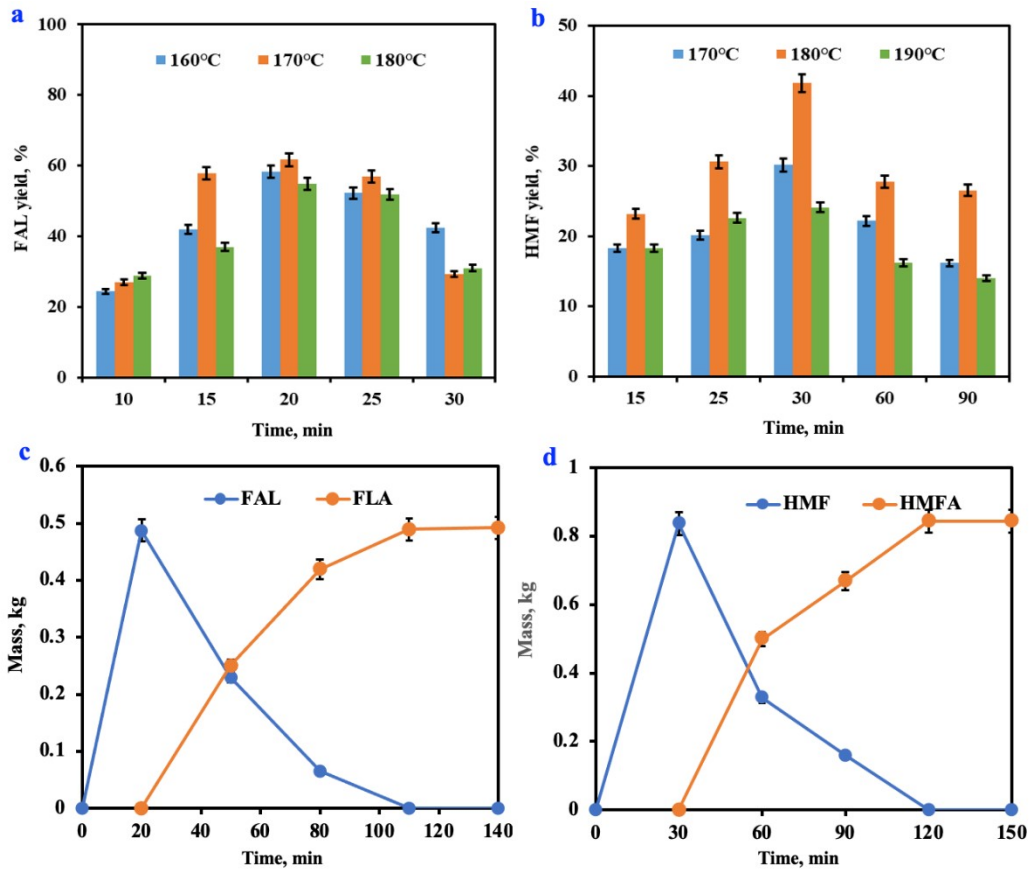

Fig. S8 Effects of time and temperature for FAL generation (a) and HMF generation (b), time courses for a one-pot chemobiocatalytic synthesis of FLA and HMFA from corncob (c) and bread crumbs (d).

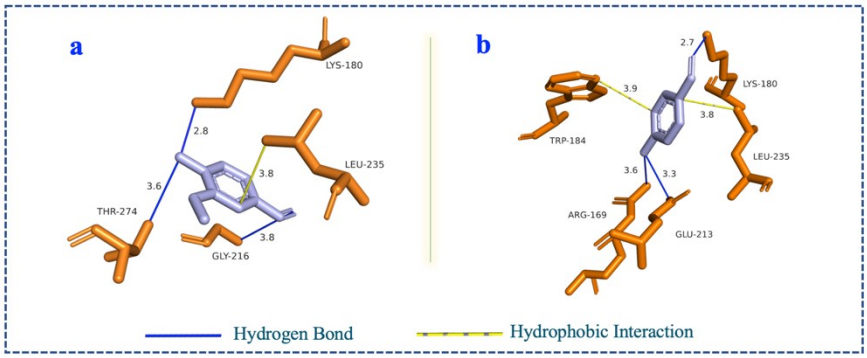

Fig. S9 The interaction of ligand [vanillin (a) and 4-hydroxybenzaldehyde (b)] with crucial residues of HNILQEND.